

Regulation of Human Vascular Endothelial Growth Factor mRNA Stability in Hypoxia by Heterogeneous Nuclear Ribonucleoprotein L*

(Received for publication, June 29, 1998, and in revised form, September 25, 1998)

Shu-Ching Shih and Kevin P. Claffey‡

From the Departments of Pathology, Beth Israel Deaconess Medical Center and Harvard Medical School, Boston, Massachusetts 02215

A 126-base region of human vascular endothelial growth factor (VEGF) 3'-untranslated region, which we identified as the hypoxia stability region, forms seven hypoxia-inducible RNA-protein complexes with apparent molecular masses ranging from 40 to 90 kDa in RNA-UV-cross-linking assays. In this study, we show that proteins that form the 60-kDa RNA-protein complex with the hypoxia stability region were present in both cytoplasmic and nuclear compartments. We purified the protein associated in the 60-kDa complex and identified it as heterogeneous nuclear ribonucleoprotein L (hnRNP L) by protein sequencing. Removal of hnRNP L by immunoprecipitation specifically abolished formation of the 60-kDa complex. Synthetic deoxyribonucleotide competition studies defined the RNA-binding site of hnRNP L as a 21-base-long sequence, 5'-CACCCACCCA-CAUACAUAU-3'. Immunoprecipitation of hnRNP L followed by reverse transcription-polymerase chain reaction showed that hnRNP L specifically interacts with VEGF mRNA in hypoxic cells *in vivo*. Furthermore, when M21 cells transfected with antisense oligodeoxynucleotide to the hnRNP L RNA-binding site, the VEGF mRNA half-life was significantly reduced under hypoxic conditions. Thus, we propose that specific association of hnRNP L with VEGF mRNA under hypoxia may play an important role in hypoxia-induced post-transcriptional regulation of VEGF mRNA expression.

Vascular endothelial growth factor (VEGF)¹, also known as vascular permeability factor, is a potent angiogenic and endothelial cell-specific mitogen (1, 2). VEGF is expressed and secreted at low levels by most normal cells but constitutively expressed at high levels by many human tumors and tumor cell lines (1–4). Hypoxia up-regulates VEGF expression and several studies have demonstrated that increase in transcription alone does not account for all of the increase in VEGF mRNA

(3–8). The post-transcriptional regulation of VEGF mRNA stability also plays a critical role in the observed hypoxic induction (6–8).

Post-transcriptional regulatory mechanisms, especially modulation of mRNA stability, has been shown to play a major role in gene expression (9). The turnover rate of a given mRNA can be determined by interactions of trans-acting factors with specific cis-element located within 3'-untranslated regions (3'-UTR) (9, 10). Many labile mRNAs, including those that encode lymphokines, cytokines, transcription factors, and proto-oncogenes, contain AU-rich elements (AREs) in their 3'-UTR (9). Identification of the interaction of AREs with trans-acting proteins has been the first step in understanding the molecular regulation of mRNA stability (9, 10). The presence of a reiterated pentamer (AUUUA)_n in many AREs has been shown to be associated with rapid mRNA turnover and translation attenuation (10–12). In the case of granulocyte-macrophage colony-stimulating factor, c-Fos, and c-Myc mRNAs, deletion of the ARE region enhances their stability, and insertion of the region into the 3'-UTR of a normally stable globin mRNA significantly destabilizes it (10–15). A variety of AUUUA-binding proteins have been identified, and examples of these include (i) a 32-kDa nuclear protein from HeLa cells (15); (ii) AU-A, AU-B, and AU-C, 30–43-kDa nuclear and/or cytoplasmic proteins from human T lymphocytes (16, 17); (iii) AUBF, a heterotrimeric protein formed by 15-, 17-, and 19-kDa subunits and present in both nucleus and cytoplasm (18, 19); and (iv) AUBP, a 36-kDa cytoplasmic protein from human spleen identified as glyceraldehyde-3-phosphate dehydrogenase (20). However, the mechanisms of how these proteins affect mRNA turnover remains unclear.

Our previous work identified a 126-base hypoxia stability region (HSR) in human VEGF 3'-UTR that is critical for the stabilization of VEGF mRNA under hypoxia (21). This region is able to form seven hypoxia-inducible mRNA-protein complexes (21). Here we report hnRNP L as a protein that interacts with the VEGF HSR and forms a hypoxia-inducible 60-kDa RNA-hnRNP L complex. The cytoplasmic hnRNP L specifically interacted with VEGF mRNA in hypoxic cells *in vivo* and regulated VEGF mRNA stability. Thus, we propose that a specific interaction of hnRNP L with VEGF mRNA may play an important role in hypoxia-induced post-transcriptional regulation of human VEGF mRNA stability.

MATERIALS AND METHODS

Antibodies and Oligodeoxyribonucleotides—Monoclonal antibodies 4D11 (anti-hnRNP L) and 4F4 (anti-hnRNP C) were generously provided by Dr. Gideon Dreyfuss (University Pennsylvania, Philadelphia) (22, 23). All of the oligodeoxyribonucleotides used in the study were synthesized from Genemed Synthesis (San Francisco, CA).

Cell Lines and Culture Conditions—Human melanoma cell line M21 was obtained from Dr. Romaine Saxton (UCLA, Los Angeles, CA). Cells

* This work was supported in part by NCI, National Institutes of Health Grant CA 64436 and by Biochem Therapeutics Inc. (Laval, Canada). The costs of publication of this article were defrayed in part by the payment of page charges. This article must therefore be hereby marked "advertisement" in accordance with 18 U.S.C. Section 1734 solely to indicate this fact.

‡ To whom correspondence should be addressed: Dept. of Pathology, Beth Israel Deaconess Medical Center and Harvard Medical School, 99 Brookline Ave., Boston, MA 02215. Tel.: 617-667-5964; Fax: 617-667-3591; E-mail: claffey@sprcore.bidmc.harvard.edu.

¹ The abbreviations used are: VEGF, vascular endothelial growth factor; HSR, hypoxia stability region; hnRNP L, heterogeneous nuclear ribonucleoprotein L; hnRNP C, heterogeneous nuclear ribonucleoprotein C; UTR, untranslated region; ARE, AU-rich element; UVXL, UV cross-linking; HPLC, high pressure liquid chromatography; PCR, polymerase chain reaction; RT-PCR, reverse transcription-PCR; PAGE, polyacrylamide gel electrophoresis.

were routinely grown in Dulbecco's modified Eagle's medium supplemented with 10% fetal bovine serum, 2 mM L-glutamine, 10 units/ml penicillin, and 10 µg/ml streptomycin. Cells were cultured under either normoxic conditions (5% CO₂, 21% O₂, 74% N₂) in a humidified Queue incubator (Asheville, NC) at 37 °C or hypoxic conditions (5% CO₂, 3% O₂, 92% N₂) in a humidified triple gas Heraeus incubator (model 6060, Hanau, Germany) at 37 °C.

Preparation of Cytoplasmic and Nuclear Extracts—Cytoplasmic and nuclear extracts were obtained as described by Claffey *et al.* (21). Following exposure to normoxia or hypoxia (3% O₂), M21 cells were washed three times in ice-cold PBS followed by lysis in 1% Triton X-100 lysis buffer containing 50 mM Hepes, pH 7.5, 10 mM sodium pyrophosphate, 150 mM NaCl, 100 mM NaF, 0.2 mM NaOAc, 1 mM EGTA, 1.5 mM MgCl₂, 10% glycerol, and 5 mM 4-(2-aminoethyl)benzene-sulfonyl fluoride (Sigma). The cytoplasmic extract was collected and centrifuged at 14,000 × *g* for 15 min, and the nuclei pellet were further extracted with the 1% Triton X-100 lysis buffer containing 400 mM NaCl for 15 min on ice. The nuclear extract was recovered after centrifuged at 14,000 × *g* for 15 min.

In Vitro Transcription—The sense and antisense HSR of human VEGF were transcribed *in vitro* as described previously (21), using T7 RNA polymerase transcription of *NotI*-linearized and T3 RNA polymerase transcription of *EcoRI*-linearized plasmid, respectively. Both biotin-UTP-labeled and [³²P]UTP-labeled RNA transcripts were generated using an RNA *in vitro* transcription kit (Stratagene, La Jolla, CA) according to the manufacturer's protocol and then treated with RNase-free DNase (Promega, Madison, WI) for 15 min at 37 °C. The [³²P]UTP-labeled transcripts were extracted once with phenol:chloroform and loaded onto RNase-free G-50 spin columns (Boehringer Mannheim) to remove free ribonucleotides. The biotin-UTP-labeled sense and antisense HSR transcripts were precipitated with ethanol and dissolved in diethyl pyrocarbonate-treated H₂O. The transcripts were then immobilized to an avidin-Sepharose 4B column (Amersham Pharmacia Biotech, Uppsala, Sweden) at 4 °C for 1 h and used in mRNA-binding protein affinity purification.

RNA Binding and UV Cross-linking (RNA-UVXL)—RNA-UVXL was performed as described earlier (21). Radiolabeled RNA transcripts (250,000 cpm/reaction) were incubated with cytoplasmic or nuclear proteins (40 µg/reaction) in 30 µl of RNA binding buffer containing 10 mM Hepes, pH 7.5, 5 mM MgCl₂, 50 mM KCl, 0.5 mM EGTA, 0.5 mM dithiothreitol, 10% glycerol, 100 µg/ml tRNA, and 5 mg/ml heparin for 20 min at 30 °C. The mixtures were UV cross-linked by UV Stratalinker (Stratagene) at room temperature for 10 min (total energy 1800 J/cm²) followed by RNase digestion (40 units of RNase T1 (Boehringer Mannheim) and 1 µg of RNase A (Sigma)) for 15 min at room temperature. The sample was then denatured in SDS-PAGE sample buffer under reducing conditions and RNA-protein complexes were analyzed by 8% SDS-PAGE and autoradiographed with Eastman Kodak Co. MR film.

Affinity Purification of mRNA-binding Proteins—Cytoplasmic extracts were prepared after M21 cells were cultured in hypoxia for 24 h. The lysate was sequentially loaded onto poly(A)-, poly(U)-, antisense HSR- and sense HSR-Sepharose 4B RNA affinity columns at room temperature. The sense HSR-Sepharose column was then extensively washed with phosphate-buffered saline, 0.2% Triton X-100. The mRNA-binding proteins were then eluted with 0.9 M NaCl and precipitated with 3 volumes of ethanol.

Immunoprecipitation—M21 cytoplasmic lysates were incubated with a 1:500 dilution of anti-hnRNP C ascites (4F4), anti-hnRNP L ascites (4D11; both 4F4 and 4D11 were obtained from Dr. Gideon Dreyfuss, University of Pennsylvania, Philadelphia, PA), or control antibody (normal mouse serum) for 2 h at 4 °C. The lysates were further incubated with 30 µl of protein A-Sepharose beads (Amersham Pharmacia Biotech) for 2 h at 4 °C. Beads were recovered by brief centrifugation, washed three times in lysis buffer, and RNA was extracted for RT-PCR or denatured directly with SDS-PAGE buffer for Western blot.

Western Blot—The immunoprecipitated material was denatured under reducing conditions, and proteins were analyzed by 8% SDS-PAGE. Western blots were performed using a 1:5000 dilution of anti-hnRNP L monoclonal antibody, anti-hnRNP C monoclonal antibody, and normal mouse serum, followed by a 1:10,000 dilution of horseradish peroxidase-conjugated goat anti-mouse IgG (Amersham Pharmacia Biotech) in a blocking buffer containing 1% bovine serum albumin and 0.1% Tween 20 in Tris-buffered saline. The blots were then developed with the ECL system (Amersham Pharmacia Biotech).

RT-PCR and Southern Blot Detection—The protein A-Sepharose-bound RNA was extracted with an equal volume of Trizol (Life Technologies, Inc.) and ½ volume of chloroform. The supernatant was collected after centrifugation at 14,000 × *g* for 15 min, and RNA was

precipitated with an equal volume of isopropyl alcohol at -80 °C for 1 h. Reverse transcription was carried out with oligo(dT) (15-mer) as primer and incubated at 42 °C for 1 h in the presence of reverse transcriptase and dNTPs (Boehringer Mannheim). The transcribed cDNA was collected after removal of free dNTPs through RNase-free G-50 spin column (Boehringer Mannheim). PCR amplification was carried out with a *Taq* DNA polymerase and two VEGF primers (VEGF 5' primer: 5'-TATGCGGATCAACCTCAC-3', corresponding to nucleotides 374–393 of VEGF coding region encoding amino acids 82–88 of the mature protein; VEGF 3' primer: 5'-ATAACATTAGCACTGTTAATTT-3', corresponding to nucleotides 435–457 3' to the translation stop codon, GenBank™ accession number AF022375) and amplified for 30 cycles. The 716-base-long PCR products were resolved by 1% agarose gel electrophoresis and detected by Southern blot with a [³²P]dCTP-labeled human VEGF165 *AccI/NotI* fragment (823 base pairs) encompassing the coding region and 330 base pairs of 3'-UTR of the full-length cDNA. Probes were prepared by the random-primed synthesis method using the Multiprime kit (Amersham Pharmacia Biotech). DNA was blotted by capillary transfer to a nylon membrane (NEN Life Science Products) in 10× SSC. Blots were cross-linked with UV Stratalinker 1800 (Stratagene), baked at 80 °C for 15 min, and prehybridized for 2–4 h at 65 °C. Hybridization was carried out overnight at 65 °C, and blots were washed at 0.5% SDS, 0.1% SSC at 55 °C before they were exposed to Kodak MR film.

Oligonucleotide Transfection and Northern Blot Detection—Antisense oligodeoxyribonucleotides, AS1 (1 µM) and AS3 (1 µM), were transfected into M21 cells by Lipofectin following the instructions of the supplier (Life Technologies, Inc.). The transfected cells were then cultured in hypoxia for 8 h, and total cellular RNA was isolated by using the RNeasy RNA extraction kit (Qiagen, Chatsworth, CA) according to the manufacturer's instructions. For the VEGF mRNA stability study, 5 µg/ml actinomycin D was added to AS1, AS3, or mock-transfected M21 cells after 6 h of hypoxia incubation. The time intervals of actinomycin D treatment were 30 min, 1 h, and 2 h, and the total hypoxia incubation time was 8 h. Total RNA was isolated and electrophoresed in 1% agarose gels containing 2.2 M formaldehyde (10 µg/lane). RNA was blotted by capillary transfer to a nylon membrane (NEN Life Science Products) in 10× SSC. Blots were cross-linked with UV Stratalinker (Stratagene), baked at 80 °C for 15 min, and prehybridized for 2–4 h at 65 °C. Hybridization was carried out overnight at 65 °C with a [³²P]dCTP-labeled human VEGF165 *AccI/NotI* fragment and GLUT-1 *BamHI* fragment (2.47 kilobase pairs). A ribosome-associated protein cDNA, 36B4, was used as a control (21). Blots were washed with 1% SDS, 1% SSC at 55 °C and exposed to Kodak MR film. VEGF was normalized to 36B4 expression using PhosphorImager analysis (Molecular Dynamics, Sunnyvale, CA).

RESULTS

Identification of VEGF 3'-HSR mRNA-binding Proteins—The post-transcriptional regulation of VEGF mRNA stability in response to hypoxia may, in part, be due to the interaction of VEGF 3'-UTR with specific binding protein(s) (6–8, 27, 28). Our previous work identified a 126-base HSR in human VEGF 3'-UTR (Fig. 1A), which is critical for hypoxia-induced human VEGF mRNA stability (21). The HSR formed seven RNA-protein complexes with M21 human melanoma cell cytoplasmic proteins with apparent molecular masses of 90, 88, 72, 60, 56, 46, and 40 kDa in RNA-UVXL (21).

Studies have shown that RNA-binding proteins are also present in nuclear compartments (15–17). Thus, we prepared both cytoplasmic and nuclear extracts from hypoxic or normoxic cultured M21 cells and compared RNA-protein complex formation by RNA-UVXL with ³²P-labeled VEGF HSR. As shown in Fig. 1B, 24-h hypoxia (3% O₂) substantially up-regulated the formation of the 90-, 88-, 72-, and 60-kDa complexes when compared with cytoplasmic extracts made from normoxic (21% O₂) cells. The 90-, 88-, 72-, and 56-kDa complexes were selectively cytoplasmic with little or no nuclear localization (Fig. 1B). Significantly higher levels of the 60-kDa complex were formed with nuclear extracts than cytoplasmic extracts, and the complex was markedly increased by hypoxia treatment in both extracts (Fig. 1B). Other than the 60-kDa complex, the nuclear extract also formed three unique complexes with ap-

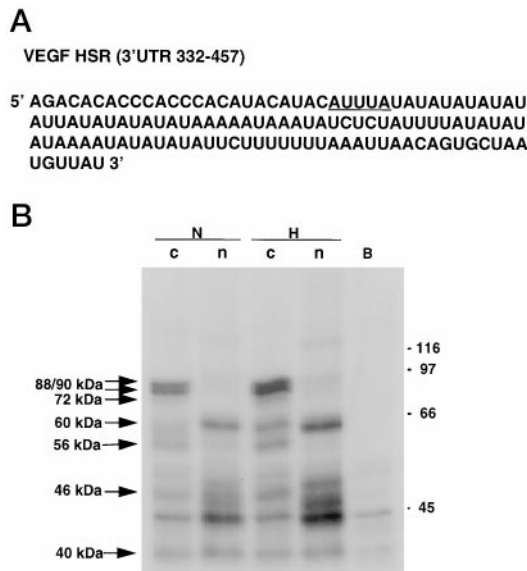


FIG. 1. VEGF HSR-binding proteins in cytoplasm and nucleus. Panel A, the human VEGF 3'-HSR (3'-UTR 332–457) sequence. The single AUUUA pentamer is underlined. Panel B, cytoplasmic (c) and nuclear (n) extracts were prepared from M21 cells cultured in normoxia (N) or 24-h hypoxia (H). The VEGF HSR RNA-protein complexes were UV-cross-linked and separated by 8% SDS-PAGE under reducing conditions. The apparent molecular masses of each RNA-protein complex are indicated by arrows. Background binding in the absence of extract is indicated as B.

parent molecular masses of 45, 48, and 120 kDa (Fig. 1B). Taken together, these results suggest that proteins that form the 90-, 80-, 72-, and 56-kDa complexes with HSR mainly appear in cytoplasm. In contrast, the protein that forms the 60-kDa complex with HSR is present in both nuclear and cytoplasmic compartments with the majority in the nucleus. Thus, given the distribution and the hypoxia induction of the 60-kDa complex, we established a protocol to purify the RNA-binding protein in the 60-kDa complex.

Purification of the RNA-binding Protein in the 60-kDa RNA-Protein Complex—The VEGF HSR is a highly AU-rich element containing 54 A bases and 52 U bases out of 126 bases, resulting in 43% A and 41% U distribution (Fig. 1A). To purify the binding protein that forms the 60-kDa complex, hypoxia-treated M21 cell lysates were loaded sequentially onto poly(A)-, poly(U)-, and antisense HSR-coupled columns to remove non-specific RNA-protein interactions prior to loading to the sense HSR-coupled column. To ensure that the protein that formed the 60-kDa complex was not removed by poly(A)-, poly(U)-, and antisense HSR-coupled columns, the flow-through from each column was collected, and RNA-UVXL was performed with ³²P-labeled HSR. As shown in Fig. 2A, the poly(A) column effectively interacted with proteins forming the 90- and 72-kDa complexes and removed them from the cell lysates, whereas the poly(U) column removed the proteins that formed the 88-, 56-, 46-, and 40-kDa complexes. Further incubation of the lysate with the antisense HSR column completely removed proteins forming the 72-kDa complex, whereas the 60-kDa complex selectively bound to the sense HSR column (Fig. 2A). These results suggest that the proteins forming the 90- and 72-kDa complexes can interact with poly(A) sequences, whereas proteins forming the 88-, 56-, 46-, and 40-kDa complexes can interact with poly(U) sequences. In contrast, the proteins present in the 60-kDa complex only specifically interact with a unique sequence in the HSR.

To analyze proteins that bound to the four mRNA columns, small aliquots of the column material were directly analyzed in

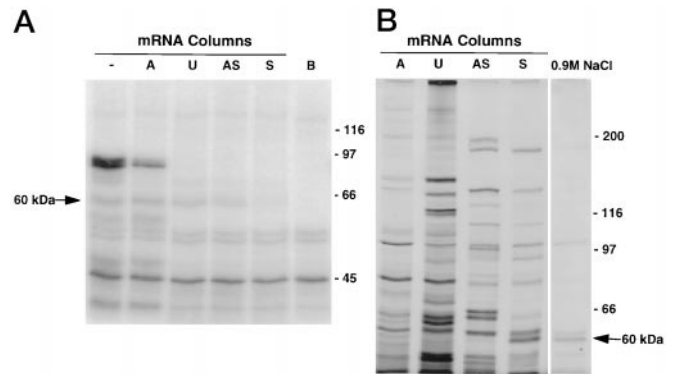


FIG. 2. Purification of RNA-binding protein that forms the 60-kDa HSR-protein complex. Panel A, M21 cytoplasmic lysates (24-h hypoxia) were sequentially loaded onto four different RNA-coupled Sepharose 4B columns: poly(A) (A), poly(U) (U), antisense HSR (AS), and sense HSR (S). Flow-through from each column was collected and used for RNA-UVXL analysis. The VEGF HSR RNA-protein complexes were analyzed by 8% SDS-PAGE. Background binding in the absence of cytoplasmic extract is indicated as B. Panel B, bound materials on each of the four columns were denatured with reducing SDS-PAGE sample buffer, separated with 6% SDS-PAGE, and visualized with silver stain. The 60-kDa sense HSR-binding protein was eluted with 0.9 M NaCl from the sense HSR column.

reducing 6% SDS-PAGE. As shown in Fig. 2B, all four mRNA columns interacted with numerous proteins. However, the sense HSR column contained one unique protein band with an apparent molecular mass near 60 kDa (indicated by an arrow). When eluted with various concentrations of NaCl, the 60-kDa protein was successfully released from the sense HSR column with 0.9 M NaCl (Fig. 2B, indicated by an arrow). The purified 60-kDa protein was then separated in a preparative 6% SDS-PAGE, stained with Coomassie Blue, and sequenced after trypsin digest and HPLC purification (Harvard Microchemistry Protein Sequencing Facility). A 16-amino acid sequence of an HPLC-purified peptide was determined as SDALETGLFLN-HYQMK, which is identical to hnRNP L, amino acid residues 522–537 (22).

The RNA-binding Protein in the 60-kDa Complex Is hnRNP L—To further confirm the RNA-binding protein in the 60-kDa complex as hnRNP L, we used anti-hnRNP L monoclonal antibody to immunoprecipitate hnRNP L from M21 cell lysates followed by detection of the 60-kDa complex formation by RNA-UVXL. For hnRNP control, anti-hnRNP C monoclonal antibody was used. Direct Western blot analysis of M21 cytoplasmic extracts showed that the anti-hnRNP L monoclonal antibody identified three proteins with apparent molecular masses of 66, 60, and 56 kDa, with the 60-kDa band being the most abundant of the three (Fig. 3A), indicating that hnRNP L is expressed as three different isoforms or differentially modified proteins in M21 cells. Anti-hnRNP L immunoprecipitation removed all of the 56- and 66-kDa bands and most of the 60-kDa hnRNP L band (Fig. 3A). Control antibodies (anti-hnRNP C and normal mouse serum) did not interact with any of the three hnRNP L proteins (Fig. 3A). Fig. 3B shows that removal of hnRNP L molecules by immunoprecipitation abolished formation of the 60-kDa RNA-protein complex in RNA-UVXL, whereas formation of the other RNA-protein complexes was unaffected. Immunoprecipitation with anti-hnRNP C did not affect any of the seven HSR-protein complexes, suggesting that hnRNP C is not one of the RNA-binding proteins present in these complexes. Taken together, these results further prove that hnRNP L is indeed the RNA-binding protein responsible for the 60-kDa RNA-protein complex. Removal of hnRNP L from cell lysates did not affect the formation of the other six RNA-protein complexes, suggesting that hnRNP L does not form specific com-

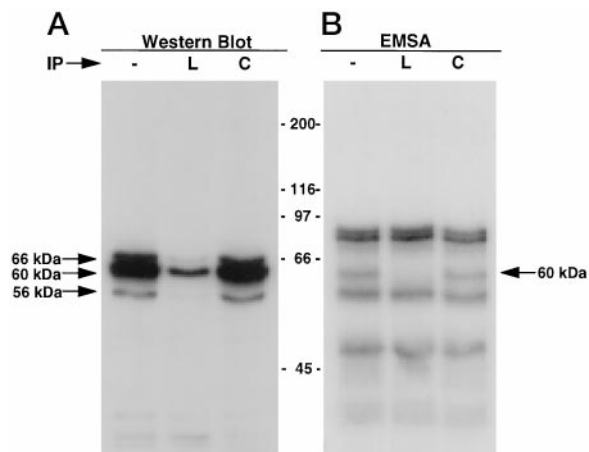


FIG. 3. hnRNP L protein is the trans-acting factor that forms the 60-kDa protein HSR complex. M21 cytoplasmic extracts (24-h hypoxia) were immunoprecipitated with anti-hnRNP L monoclonal antibody (L), anti-hnRNP C monoclonal antibody (C), or normal mouse serum (-). The unbound proteins after immunoprecipitation were either analyzed by Western blot with anti-hnRNP L monoclonal antibody (A) or RNA-UVXL with 32 P-labeled VEGF HSR (B). The samples from both experiments were separated with 8% SDS-PAGE.

plexes with other RNA-binding proteins interacting with VEGF HSR.

Hypoxia Regulation of hnRNP Expression—Hypoxia substantially increases the steady state level of VEGF mRNA (4–8). The formation of hnRNP L-VEGF 3'-HSR complex markedly increased when cytoplasmic protein extracts were obtained from M21 cells exposed to hypoxia (3% O₂) as compared with those exposed to normoxia (21% O₂) (Fig. 1B). Thus, it was of interest to compare the effect of hypoxia on synthesis and distribution of hnRNP L in nuclear *versus* cytoplasmic compartments. As shown in Fig. 4, M21 cells grown in normoxic conditions contained high levels of hnRNP L, especially in the nuclear compartment. A minor induction of hnRNP L can be seen under hypoxia in both cytoplasm and nucleus, with the 56-kDa immunoreactive band in cytoplasm being the most significantly increased (Fig. 4). Conversely, the hnRNP C level in cytoplasm decreased to an undetectable range after a 24-h hypoxia incubation, although it remained high in the nucleus (Fig. 4). These results suggest that hypoxia differentially regulates the distribution of hnRNPs in different cellular compartments.

Identification of hnRNP L mRNA Binding Site—To define the hnRNP L mRNA binding site, six antisense oligodeoxyribonucleotides were synthesized from different regions of the HSR (Fig. 5A, AS1–AS6). To ensure the stability of oligonucleotides in the RNA-UVXL, we synthesized oligodeoxyribonucleotides instead of oligoribonucleotides. As shown in Fig. 5B, AS1 (1 μ M) efficiently blocked the interaction of hnRNP L with 32 P-labeled HSR and abolished formation of the 60-kDa RNA-hnRNP L complex. The blocking of HSR-hnRNP L complex formation can be seen as low as 0.05 μ M AS1 (data not shown). AS6 abolished the formation of the 90- and 88-kDa complexes and partially inhibited the HSR-hnRNP L complex, whereas AS2, AS3, AS4, and AS5 did not show any effect (Fig. 5B). These results suggest that the complementary region of AS1 on HSR contains the hnRNP L binding site and that hnRNP L interacts with the single-stranded mRNA region. AS1 and AS6 lack sequence homology; thus, the partial inhibition of hnRNP L interaction with HSR observed with AS6 may be functioning by blocking the 90- and 88-kDa complexes that may promote hnRNP L binding in some manner.

To further explore the hnRNP L mRNA binding site, we chemically synthesized the sense oligodeoxyribonucleotide

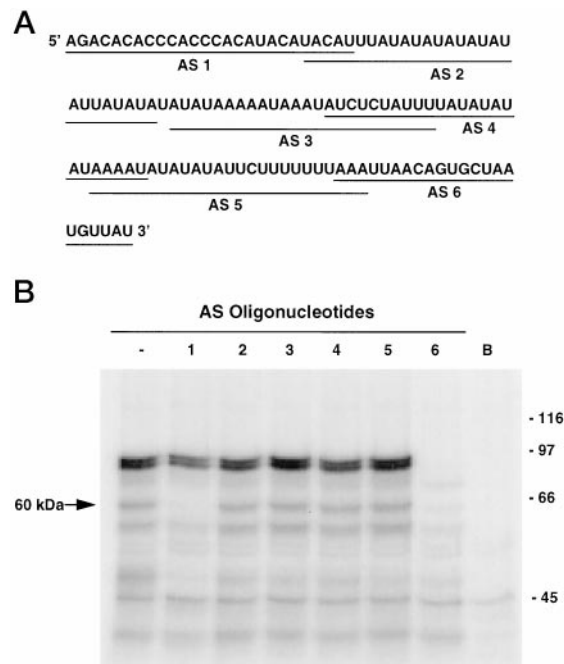


FIG. 4. Regulation of hnRNP L and hnRNP C expression by hypoxia. Cytoplasmic (c) and nuclear (n) extracts were prepared from M21 cells after culture in normoxia (N) or 24-h hypoxia (H). Proteins were separated by 8% SDS-PAGE, and Western blot was performed with anti-hnRNP L (L) or anti-hnRNP C (C) monoclonal antibodies. Arrows indicate hnRNP L and hnRNP C proteins.

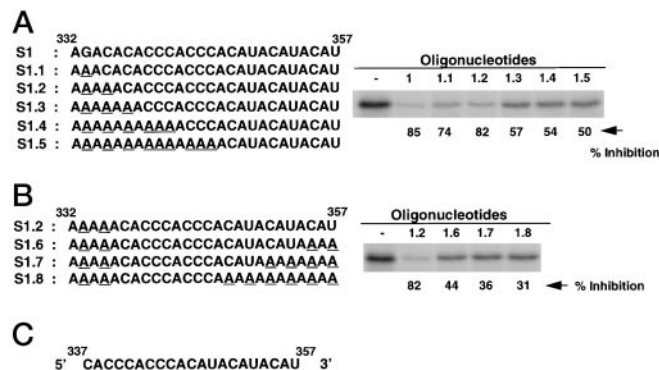


FIG. 5. Inhibition of the 60-kDa HSR-hnRNP L complex formation with antisense oligodeoxyribonucleotides. A, VEGF HSR sequence and the location of six chemically synthesized antisense (AS) oligodeoxyribonucleotides. B, blocking of HSR and hnRNP L interaction by AS oligodeoxyribonucleotides. M21 cytoplasmic extracts (24-h hypoxia) were used for RNA-UVXL in the absence (-) or presence of each of the six AS oligodeoxyribonucleotides (1 μ M). RNA-protein complexes were detected by 8% SDS-PAGE. Background binding in the absence of extract is indicated as B.

(S1), which was complementary to AS1 (Fig. 6A) and attempted to compete for hnRNP L binding to 32 P-labeled HSR. As shown in Fig. 6A, S1 (10 μ M) successfully competed with 32 P-labeled HSR for hnRNP L binding and substantially reduced HSR-hnRNP L complex formation (85% inhibition of hnRNP L binding). The competition of S1 for hnRNP L binding to HSR can be seen as low as 0.1 μ M AS1 (data not shown). To define the hnRNP L binding site, eight different oligodeoxyribonucleotides were synthesized after modification of the internal base sequences of S1 (Fig. 6). As shown in Fig. 6A, substitution of base 333 G to A in S1.1 or further substitution of base 335 C to A in S1.2 showed strong competition for hnRNP L binding to the 32 P-labeled HSR (S1.1 and S1.2 showed 74 and 82% inhibition, respectively), thus demonstrating that neither 333 G or 335 C were required for hnRNP L binding. However, substitu-

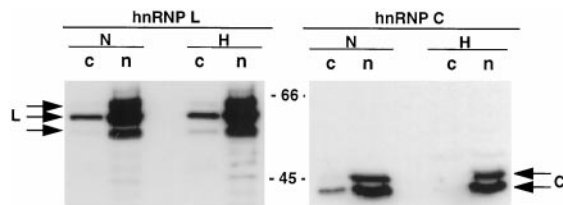


FIG. 6. Identification of hnRNP L binding site on HSR. S1 is a sense-orientated oligodeoxyribonucleotide that is complementary to AS1 and comprises bases 332–357 of the HSR. **A**, competitive RNA-UVXL with sense (S) oligodeoxyribonucleotides with modifications in the 5'-end. Competitive RNA-UVXL was performed with ^{32}P -labeled VEGF HSR and M21 cytoplasmic extract (24-h hypoxia) in the absence (–) or presence of S1 or its derivatives (10 μM). Band intensities of the 60-kDa HSR-hnRNP L complex were quantified by PhosphorImager analysis. The percent inhibition was calculated as the percentage decrease in band intensity compared with control (–). **B**, competitive RNA-UVXL with sense oligodeoxyribonucleotides with 3' modifications. **C**, minimal defined 21-base binding site for hnRNP L-VEGF HSR binding.

tion of base 337 C to A in S1.3 showed a substantial reduction in the ability to compete for hnRNP L binding (Fig. 6A, 57% inhibition), and any modifications after base 337 showed a similar affect (Fig. 6A; S1.4 and S1.5 showed 54 and 50% inhibition, respectively). These results suggest that bases 332–336 (AGACA) in S1 are not essential for hnRNP L binding and that S1.2 contains the hnRNP mRNA binding site.

The S1.2 oligodeoxyribonucleotide has three ACAU repeats. To study the potential importance of the ACAU repeats for hnRNP L binding, three oligodeoxyribonucleotides (S1.6, S1.7, and S1.8) with 1–3 ACAU repeats were synthesized (Fig. 6B). As shown in Fig. 6B, removal of any one of the ACAU repeats from S1.2 substantially reduced the ability to compete for hnRNP L binding with ^{32}P -labeled HSR (S1.6, S1.7, and S1.8 showed only 44, 36, and 31% inhibition, respectively). This result suggests that all three ACAU repeats are essential for hnRNP L binding. Overall, these results suggest that the minimal hnRNP L mRNA binding site appears to be $^{337}\text{CACCCAC-CCACAUACAUAUACA}^{357}$. Using a GenBankTM Blast search, this 21-base sequence was only found in human and bovine VEGF 3'-UTRs but not in other VEGF species or other genes.

The hnRNP L Interacts with VEGF mRNA in Hypoxic Cells *in Vivo*—To determine if hnRNP L interacts with VEGF mRNA *in vivo*, we immunoprecipitated hnRNP L with anti-hnRNP L monoclonal antibody from 24-h hypoxia-cultured M21 cell lysates and performed RNA extraction, RT-PCR, and Southern blot detection. The VEGF primers used in RT-PCR contained part of the VEGF coding region and the entire 3'-HSR and should produce a 716-base VEGF165 isoform product. As shown in Fig. 7A, a unique PCR product of approximately 700 base pairs in length appeared with hnRNP L immunoprecipitation, whereas immunoprecipitates for hnRNP C and normal mouse serum control antibodies did not show any distinct band in the same region. Southern blot hybridization with VEGF cDNA probe showed a strong hybridization to the hnRNP L PCR product, thus confirming the PCR product as VEGF cDNA (Fig. 7B). A weak interaction of VEGF cDNA probe with the hnRNP C PCR product was observed, whereas the normal mouse serum control did not have any detectable signal (Fig. 7B). Studies have shown that hnRNP C can interact with the poly-U region of mRNAs (30), and thus it is possible that hnRNP C is associating with many mRNAs including VEGF *in vivo*. Taken together, these results verify that hnRNP L interacts with VEGF mRNA in hypoxic cells *in vivo*.

Interaction of hnRNP L and VEGF mRNA Is Important for VEGF mRNA Stability—To study whether hnRNP L plays an important role in the regulation of VEGF mRNA expression,

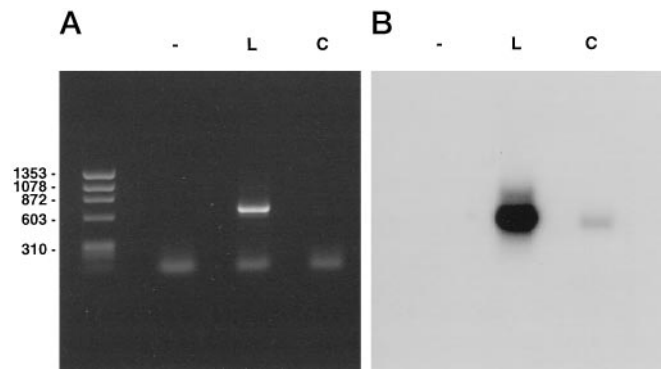


FIG. 7. Interaction of hnRNP L with VEGF mRNA in hypoxic cells *in vivo*. M21 cytoplasmic extracts (24-h hypoxia) were immunoprecipitated with anti-hnRNP L monoclonal antibody (L), anti-hnRNP C monoclonal antibody (C), or normal mouse serum (–). The co-immunoprecipitated mRNAs were extracted and used as templates for RT-PCR. The PCR products were resolved by 1% agarose gel electrophoresis (A) and detected by Southern blot with a ^{32}P [dCTP]-labeled human VEGF (B).

M21 cells were transfected with antisense oligodeoxyribonucleotide AS1 to block interaction of hnRNP L with VEGF mRNA in hypoxic cells *in vivo*. The AS3 oligodeoxyribonucleotide, which did not block the formation of any HSR-protein complex formation (Fig. 5), was used as control. As shown in Fig. 8, M21 cells transfected with AS1 had substantially lower levels of VEGF mRNA when compared with mock-transfected control cells (54.3% by PhosphorImager analysis), whereas the GLUT-1 mRNA level was not affected by the transfection (97.3%), indicating that AS1 is specifically affecting VEGF mRNA expression. The control oligodeoxyribonucleotide AS3-transfected cells did not show changes for either VEGF mRNA (109.5%) or GLUT-1 mRNA (94.5%). These results suggest that blocking of hnRNP L and VEGF mRNA interaction *in vivo* will specifically affect VEGF mRNA accumulation in hypoxia.

The hnRNPs are a family of abundant nuclear proteins that are involved in pre-mRNA processing and splicing (22–24). To address whether the effect of AS1 repression of VEGF mRNA accumulation is through VEGF mRNA stability, we transfected M21 cells with AS1, AS3, or mock reagent and examined VEGF mRNA decay under hypoxic conditions. The rate of decay of the mature VEGF mRNA was determined by Northern blot hybridization after treatment of cells with the transcriptional inhibitor actinomycin D. As shown in Fig. 9A, M21 cells transfected with AS1 showed a substantial decrease in VEGF mRNA level after 30 min of actinomycin D treatment, whereas mock- and AS3-transfected cells maintained higher VEGF levels for up to 1 h of actinomycin D treatment. Conversely, GLUT-1 mRNA did not show any changes by AS1 when compared with mock- and AS3-transfected cells (Fig. 9A). When the VEGF mRNA decay curve of a triplicate assay was plotted over a 2-h actinomycin D treatment and VEGF mRNA half-life ($t_{1/2}$) was measured, AS1-transfected cells showed a half-life of 32 ± 5.7 min, whereas mock- and AS3-transfected cells showed half-lives of 53 ± 4.1 and 57 ± 5.6 min, respectively (Fig. 9B). AS1-transfected cells showed statistically significant differences ($p \leq 0.0005$) in VEGF mRNA levels when compared with mock-transfected cells at both 30 and 60 min. These results suggest that blocking of the hnRNP L and VEGF mRNA interaction decreases VEGF mRNA stability under hypoxia. These also suggest that although hnRNP L is important for mRNA processing, interaction of hnRNP L with VEGF mRNA 3'-UTR plays a critical role in post-transcriptional regulation of VEGF mRNA stability.

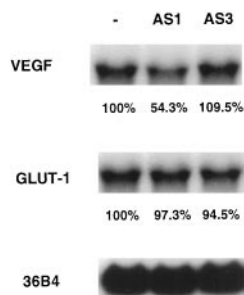


FIG. 8. Blocking of hnRNP L and VEGF mRNA interaction reduces steady state VEGF mRNA level. M21 cells were transiently transfected in the absence (-) or presence of 1 μ M AS1 or AS3 oligodeoxynucleotides, and VEGF, GLUT-1, and 36B4 mRNA levels were detected by Northern blot analysis. VEGF and GLUT-1 mRNA signals were normalized with the ribosome-associated mRNA, 36B4, from each lane and quantified by PhosphorImager. The mRNA from AS1- and AS3-transfected cells were calculated as percentage of VEGF or GLUT-1 of mock-transfected mRNA (-) signals designated as 100%.

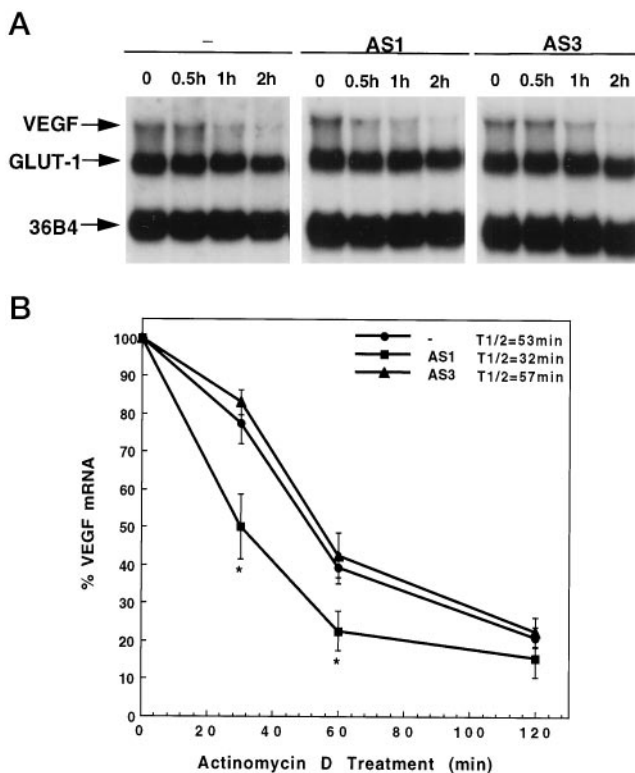


FIG. 9. Blocking of hnRNP L and VEGF mRNA interaction by AS1 oligodeoxynucleotide decreases VEGF mRNA stability. M21 cells were transiently transfected in the absence (-) or presence of 1 μ M AS1 or AS3 oligodeoxynucleotide, and VEGF mRNA stability was analyzed in an 8-h hypoxia assay. Actinomycin D (5 μ g/ml) was periodically added beginning at 6 h hypoxia and incubated for 2, 1, or 0.5 h, respectively, to triplicate plates. Total mRNA was extracted, and VEGF, GLUT-1, and 36B4 mRNA levels were detected by Northern blot. A, representative Northern blot analysis of VEGF mRNA level after actinomycin D treatment. B, VEGF mRNA decay curves and mRNA half-life ($t_{1/2}$). VEGF mRNA signal was normalized with the ribosome-associated mRNA, 36B4, from each lane after quantification by PhosphorImager and calculated mean \pm S.D. from a triplicate experiment. VEGF mRNA signal without actinomycin D treatment was defined as 100%, and actinomycin D treated VEGF mRNA levels were calculated as percentage of decay. The asterisk indicates $p \leq 0.0005$ when AS1- and mock (-) transfected cells were compared at 30- and 60-min actinomycin D treatment using Student's t test.

DISCUSSION

With a half-life of only 30–45 min under normal growth conditions (6–8), VEGF mRNA falls within a class of labile mRNAs encoding for many transiently expressed proteins in-

cluding cytokines, lymphokines, oncogenes, and transcriptional activators (9). The mechanisms whereby normally labile mRNAs are stabilized by stimuli such as hypoxia, growth stimulation, and viral infection are unclear. On the basis of RNA-binding and UV cross-linking, the interaction of specific cellular proteins with mRNAs have been shown to be altered in response to stimuli, which correlates with changes in mRNA stability (9–21). This has led to the hypothesis that mRNA turnover is mediated principally through mRNA-binding proteins that specifically recognize AREs and other sequence motifs.

Our previous work demonstrated a 126-base HSR in human VEGF 3'-UTR, which is responsible for hypoxia-induced VEGF mRNA stability and forms seven hypoxia-inducible RNA-protein complexes with M21 human melanoma cell extracts (21). In the present study, we showed that the protein that forms the 60-kDa RNA-protein complex is present in both nuclear and cytoplasmic compartments (Fig. 1). Protein sequencing and immunodepletion studies identified that protein in the 60-kDa RNA-protein complex as heterogeneous nuclear ribonucleoprotein L (hnRNP L) (Figs. 3 and 4). The specific mRNA binding site of hnRNP L was identified as 3'-CACCCACCAUCAUCAUCAU-5', a 21-base single-stranded element, which is unique to human and bovine VEGF 3'-UTR sequences (Figs. 5 and 6). Immunoprecipitation of hnRNP L followed by RT-PCR showed that hnRNP L specifically interacted with VEGF mRNA in hypoxic cells *in vivo* (Fig. 7). Furthermore, when M21 cells were transfected with antisense oligodeoxynucleotide to the hnRNP L RNA-binding site, the hypoxia-induced VEGF mRNA half-life decreased from 53 ± 4.1 min to 32 ± 5.7 min (Fig. 8). This study identifies for the first time that hnRNP L as a protein present in human cells that is capable of interacting with VEGF mRNA 3'-UTR and is functionally involved in the post-transcriptional regulation of VEGF mRNA under hypoxic conditions.

It is well documented that unstable mRNAs containing AREs generally consists of either scattered AUUUA pentanucleotides, contiguous AUUUA repeats, nonamer motif UUAUUUA(U/A)(U/A), or a stretch of AU residues lacking either motif (10–15). These AREs interact with cytoplasmic and/or nuclear proteins and usually form ARE-protein complex with average molecular mass less than 40-kDa (10, 15–20). The VEGF HSR is also a highly AU-rich element (43% A and 41% U) and contains one AUUUA pentanucleotide as well as two stretches of AU residues. However, interaction of the HSR with cellular proteins formed seven RNA-protein complexes with higher molecular masses (ranging from 40 to 90 kDa). The HSR also formed same protein complexes with five other cell lines we tested (data not shown), indicating that those RNA-binding proteins are common proteins to different cell lines. The 3'-UTRs of two other hypoxia up-regulated genes, erythropoietin (25) and tyrosine hydroxylase (26), interacted with mRNA-binding proteins with apparent molecular masses ranging from 66 to 140 kDa. However, the VEGF HSR and the 3'-UTRs of both erythropoietin and tyrosine hydroxylase lack significant homology. Moreover, the interaction site for a 66-kDa protein to tyrosine hydroxylase 3'-UTR is different from the hnRNP L mRNA binding site. Thus, VEGF HSR-binding proteins may be distinct from those that recognize other hypoxia-inducible genes.

Studies of rat VEGF mRNA demonstrated a 600-base region covering nucleotides 1251–1877 in the 3'-UTR required for rat VEGF mRNA stability (27, 28). However, little homology exists between the human VEGF HSR sequence and the rat 600-base region. In addition, the protein complexes observed by EMSA in the rat ARE-binding proteins are 17, 28, and 34 kDa (27, 28),

none of which correlate to the hypoxia-induced complexes described here. Recent studies identified that the 34-kDa rat VEGF ARE-binding protein as HuR, which interacted with a 45-base element of rat VEGF 3'-UTR and stabilized the mRNA under hypoxia (28). This element is also present in the human 3'-UTR covering nucleotides 1682–1726 3' to the translation stop codon, a region close to the poly(A) tail. Taken together, these studies suggest that there are a variety of mRNA-binding proteins present in cells, and the regulation of mRNA turnover probably depends on the mRNA sequences, the metabolic and activation state of the cells, and the regulation of the RNA-binding protein expression and distribution.

The hnRNPs are a family of abundant nuclear proteins that are involved in pre-mRNA processing and splicing (22–24). The hnRNP L differs from other ARE-binding hnRNPs in that hnRNP A, hnRNP C, and hnRNP D interact with the AUUUA motif and may participate in mRNA destabilization (15, 29–32), whereas hnRNP L interacts with a unique sequence in the human and bovine VEGF 3'-UTR (3'-CACCCACCCACAUA-CAUACAU-5') and probably has a predominant stabilization effect. In support of this hypothesis, hypoxia substantially increased hnRNP L in both nucleus and cytoplasmic compartments, whereas hnRNP C was dramatically decreased to undetectable levels in the cytoplasm after a 24-h hypoxic treatment. This differential regulation of hnRNPs under hypoxia, a decrease in the hnRNP C and an increase in the hnRNP L in cytoplasm, may define a key balance regulating mRNA metabolism during metabolic stress. The 21-base-long mRNA binding site of hnRNP L is juxtaposed to the only AUUUA pentanucleotide and a long stretch of AU residues. Therefore, it is possible that the interaction of hnRNP L may block other proteins such as hnRNP C from interacting with and destabilizing the mRNA. Furthermore, under hypoxia we observe increased expression of hnRNP L and the specific interaction of hnRNP L with VEGF mRNA *in vivo*, along with reduced VEGF mRNA stability observed with transfection of antisense oligodeoxynucleotide to the hnRNP L binding site. Thus, hnRNP L appears to play a significant role in the post-transcriptional regulation of VEGF mRNA during hypoxic stress.

Using Western blot analysis, anti-hnRNP L monoclonal antibody identified three proteins with apparent molecular masses of 66, 60, and 56 kDa, with the cytoplasmic 56-kDa protein being the most strongly up-regulated by hypoxia. Since there was only one RNA-hnRNP L complex formed in RNA-UVXL, it is unlikely that all three hnRNP L isoforms interacted with HSR. Interaction of hnRNP L with the entire 21-base binding site would account for approximately 6 kDa of the 60-kDa HSR-hnRNP L complex after UV-cross-linking and RNase treatment. Thus, it is reasonable to predict that the 56-kDa hnRNP L isoform is the molecule that is specifically interacting with HSR. Comparing the minor induction of hnRNP L levels in hypoxia by Western blot to the marked increase of hnRNP L and HSR interaction in RNA-UVXL assays leads us to speculate that post-translational modification of hnRNP L isoforms may promote a higher hnRNP L binding affinity to HSR under hypoxia, an interesting possibility we are currently investigating.

To effectively define the complex cellular mechanisms that control mRNA stability such as VEGF, identification of the mRNA-binding proteins is required. Purification and identification of hnRNP L protein as one of the VEGF mRNA-binding proteins is a significant step in defining the molecular regula-

tion of VEGF mRNA expression under hypoxic conditions. Here we have detailed the characterization of hnRNP L as one of the hypoxia-inducible RNA-binding proteins that recognizes a specific region of the human VEGF HSR. The potential signaling mechanisms that regulate hnRNP L isoform expression and association with VEGF mRNA can now be investigated in detail. Since a complex of at least seven proteins bind to VEGF HSR, interaction of hnRNP L with other proteins in the same complex may be required to protect the VEGF mRNA from nuclease digestion. Interference of hnRNP L binding to VEGF HSR significantly affected VEGF mRNA expression in hypoxia, indicating that it plays an important and novel role in VEGF expression under hypoxic stress. Identification of the other mRNA-binding proteins that recognize VEGF HSR, how they are regulated, and their potential interaction with hnRNP L will be necessary to get a complete understanding of the molecular mechanisms resulting in hypoxia-mediated VEGF mRNA stability.

Acknowledgments—We thank Dr. Gideon Dreyfuss for providing antibodies against hnRNP L and hnRNP C. We are grateful to Andrew Mullen and Kristin Abrams for helpful technical assistance.

REFERENCES

1. Leung, D. W., Cachianes, G., Kuang, W.-J., Goeddel, D. V., and Ferrara, N. (1989) *Science* **246**, 1306–1309
2. Senger, D. R., Van De Water, L., Brown, L. F., Nagy, J. A., Yeo, K.-T., Yeo, T.-K., Berse, B., Jackman, R. W., Dvorak, A. M., and Dvorak, H. F. (1993) *Cancer Metastasis Rev.* **12**, 303–324
3. Shweiki, D., Itin, A., Soffer, D., and Keshet, E. (1992) *Nature* **359**, 843–845
4. White, F. C., Carroll, S. M., and Kamps, M. P. (1995) *Growth Factors* **12**, 289–301
5. Levy, A. P., Levy, N. S., Wegner, S., and Goldberg, M. A. (1995) *J. Biol. Chem.* **270**, 13333–13340
6. Shima, D. T., Deutsch, U., and D'Amore, P. A. (1995) *FEBS Lett.* **370**, 203–208
7. Stein, I., Neeman, M., Shweiki, D., Itin, A., and Keshet, E. (1995) *Mol. Cell. Biol.* **15**, 5363–5368
8. Levy, A. P., Levy, N. S., and Goldberg, M. A. (1996) *J. Biol. Chem.* **271**, 2746–2753
9. Ross, J. (1995) *Microbiol. Rev.* **59**, 423–450
10. Chen, C.-Y. A., and Shyu, A.-B. (1995) *Trends Biochem. Sci.* **20**, 465–470
11. Shaw, G., and Kamen, R. (1986) *Cell* **46**, 659–667
12. Caput, D., Beutler, B., Hartog, K., Thayer, R., Brown-Shimer, S., and Cerami, A. (1986) *Proc. Natl. Acad. Sci. U. S. A.* **83**, 1670–1674
13. Shyu, A.-B., Greenberg, M. E., and Belasco, J. G. (1989) *Genes Dev.* **3**, 60–72
14. Wilson, T., and Treisman, R. (1988) *Nature* **336**, 396–399
15. Vakalopoulou, E., Schaack, J., and Shenk, T. (1991) *Mol. Cell. Biol.* **11**, 3355–3364
16. Bohjanen, P. R., Petryniak, B., June, C. H., Thompson, C. B., and Lindsten, T. (1991) *Mol. Cell. Biol.* **11**, 3288–3295
17. Bohjanen, P. R., Petryniak, B. P., June, C. H., Thompson, C. B., and Lindsten, T. (1992) *J. Biol. Chem.* **267**, 6302–6309
18. Malter, J. S. (1989) *Science* **246**, 664–666
19. Gillis, P., and Malter, J. S. (1991) *J. Biol. Chem.* **266**, 3172–3177
20. Nagy, E., and Rigby, W. F. C. (1995) *J. Biol. Chem.* **270**, 2755–2763
21. Claffey, K. P., Shih, S.-C., Mullen, A., Dziennis, S., Cusick, J. L., Abrams, K. R., Lee, S. W., and Detmar, M. (1998) *Mol. Biol. Cell* **9**, 469–481
22. Pinol-Roma, S., Swanson, M. S., Gall, J. G., and Dreyfuss, G. (1989) *J. Cell Biol.* **109**, 2575–2587
23. Liu, X., and Mertz, J. E. (1995) *Genes Dev.* **9**, 1766–1780
24. Dreyfuss, G., Matunis, M. J., Pinol-Roma, S., and Burd, C. G. (1993) *Annu. Rev. Biochem.* **62**, 289–321
25. Rondon, I. J., MacMillan, L. A., Beckman, B. S., Goldberg, M. A., Schneider, T., Bunn, H. F., and Malter, J. S. (1991) *J. Biol. Chem.* **266**, 16594–16598
26. Czyzyk-Krzeska, M. F., Dominski, Z., Kole, R., and Millhorn, D. E. (1994) *J. Biol. Chem.* **269**, 9940–9945
27. Levy, A. P., Levy, N. S., and Goldberg, M. A. (1996) *J. Biol. Chem.* **271**, 25492–25497
28. Levy, N. S., Chung, S., Furneaux, H., and Levy, A. P. (1998) *J. Biol. Chem.* **273**, 6417–6423
29. Brewer, G. (1991) *Mol. Cell. Biol.* **11**, 2460–2466
30. Hamilton, B. J., Nagy, E., Malter, J. S., Arrick, B. A., and Rigby, W. F. C. (1993) *J. Biol. Chem.* **268**, 8881–8887
31. Zhang, W., Wagner, B. J., Ehrenman, K., Schaefer, A. W., DeMaria, C. T., Crater, D., DeHaven, K., Long, L., and Brewer, G. (1993) *Mol. Cell. Biol.* **13**, 7652–7665
32. Kiledjian, M., DeMaria, C. T., Brewer, G., and Novick, K. (1997) *Mol. Cell. Biol.* **17**, 4870–4876